Shell/core structure and magnetic properties of carbon-coated Fe-Co(C) nanocapsules

2001 J. Phys.: Condens. Matter 13 1921

(http://iopscience.iop.org/0953-8984/13/9/314)

INSTITUTE OF PHYSICS PUBLISHING JOURNAL OF PHYSICS: CONDENSED MATTER

J. Phys.: Condens. Matter **13** (2001) 1921–1929 www.iop.org/Journals/cm PII: S0953-8984(01)18562-0

Shell/core structure and magnetic properties of carbon-coated Fe–Co(C) nanocapsules

Z D Zhang[1,6], J G Zheng[2], I Skorvanek[3], G H Wen[4], J Kovac[3], F W Wang[4], J L Yu[1], Z J Li[5], X L Dong[1,5], S R Jin[5], W Liu[1] and X X Zhang[4]

[1] International Centre for Materials Physics, Institute of Metal Research, Academia Sinica, Shenyang 110015, People's Republic of China
[2] Department of Engineering, University of Liverpool, Ashton Street, Liverpool L69 3GH, UK
[3] Institute of Experimental Physics, Slovak Academy of Sciences, 04353 Kosice, Slovakia
[4] Department of Physics, Hong Kong University of Science and Technology, Clearwater Bay, Kowloon, Hong Kong, People's Republic of China
[5] Laboratory of Ultrafine Particles, Shenyang Polytechnic University, Shenyang 110023, People's Republic of China

E-mail: zdzhang@imr.ac.cn (Z D Zhang)

Received 30 October 2000, in final form 11 January 2001

Abstract

Shell–core structures of Fe(C), Co(C) and Fe–Co(C) nanocapsules, prepared by an arc discharge process in a mixture of methane and helium, have been demonstrated by means of high-resolution transmission electron microscopy (HRTEM). These nanoscale magnetic cores are protected by graphite shells. It has been found that the zero-field-cooled (ZFC) magnetization of Fe–Co(C) nanocapsules that display different characteristics in three temperature ranges can be well interpreted in terms of the unblocking of magnetization of small single-domain particles and the depinning of large multidomain particles. The saturation magnetization of these nanocapsules decreases monotonically, while the coercivity decreases significantly with increasing temperature.

1. Introduction

Since the discovery [1] and preparation [2] in macroscopic quantities of C_{60}, there have been extensive investigations on fullerenes [1, 2], carbon nanotubes [3, 4], carbon-coated nanocapsules and a wide range of carbon-based materials [5, 6]. Recently, we successfully fabricated carbon-encapsulated magnetic nanocapsules by an arc discharge process in a methane (CH_4) atmosphere, where a carbon rod served as the cathode and a metal or alloy block as the anode [7, 8]. In this paper, we give direct evidence for the formation of a shell–core structure of Fe(C), Co(C), Fe–Co(C) nanocapsules using high-resolution transmission electron microscopy (HRTEM). The temperature dependences of their magnetizations reveal a very wide energy barrier distribution due to a wide distribution of particle size.

[6] Author to whom any correspondence should be addressed. Telephone: 86-24-23843531; fax: 86-24-23891320.

2. Experimental details

Fe–Co(C) nanocapsules were prepared by the arc discharge process [7, 8]. The $Fe_{70}Co_{30}$ alloy to be evaporated served as the anode, while a carbon rod served as the cathode. As the reactant gas and a source of hydrogen plasmas, a mixture of 30% methane (CH_4) and 70% helium was introduced into the evacuated chamber until the gas pressure in the chamber reached 100 Torr. When a voltage of 20–30 V was applied, the Fe–Co alloy was evaporated while CH_4 decomposed into C and H. Fe(C) and Co(C) nanocapsules were produced by the same process, except that Fe and Co blocks served as anodes, respectively. These nanocapsules were collected from the water-cooled wall of the chamber for different experiments. TEM samples were prepared in two steps: (a) the nanocapsules were first dispersed in ethyl alcohol by an ultrasonic field; and (b) a drop of the suspension was then allowed to evaporate onto a carbon-coated TEM mesh grid. The morphologies of the nanocapsules were observed using a JEOL 2000EX HRTEM operating at 200 kV. Their magnetization was measured in the temperature range from 4.2 to 350 K, either by using a superconducting quantum interference device (SQUID) magnetometer or by a VSM equipped with a superconducting coil with the maximum magnetic field of 5 T.

3. Results and discussion

Lattice images with interplanar spacings larger than 0.17 nm can be easily obtained using the JEOL 2000EX HRTEM, from which crystalline phases can be identified. Figure 1 shows three HRTEM images recorded from Fe(C), Co(C) and Fe–Co(C) particles. The common structural feature of all three kinds of particle is the capsule morphology—that is, each particle is composed of a core and a shell. All shell layers are characterized by curved lattice fringes of interplanar spacing 0.34 nm corresponding to the (0002) lattice plane of graphite. This suggests that these shells are graphitic carbon. The average shell thicknesses of the Fe(C), Co(C) and Fe–Co(C) capsules are 2.0 nm, 1.0 nm and 3.4 nm, respectively. No other type of shell is observed by means of HRTEM. X-ray diffraction (XRD) spectra (figures 2(a) and 2(c)) of Fe(C) and Fe–Co(C) capsules also show the graphite-related peak at $2\theta = 26^\circ$ corresponding to $d = 0.34$ nm. No diffraction peak occurs at $2\theta = 26^\circ$ in the XRD spectrum (figure 2(b)) of Co(C) capsules. This is because Co(C) shells are too thin to give rise to a detectable XRD peak.

It has been proved that the graphite shells can protect nanocapsules from oxidation [7, 8]. No peak of the oxides is observed in the XRD patterns shown in figure 2. X-ray photoelectron spectra (XPS) revealed that the shell of the Fe–Co(C) nanocapsules does not contain oxygen, and protects the particles from oxidation. The contents of oxygen determined by an oxygen measurement system are 3.60 and 0.72 wt% for the Fe–Co ultrafine particles and the Fe–Co(C) nanocapsules, respectively [7, 8]. The magnetization of the Fe–Co(C) nanocapsules is higher than that of the Fe–Co ultrafine particles, because there is less oxidation in the former case [7, 8].

HRTEM lattice images indicate that the core phases are bcc α-Fe(C) and orthorhombic Fe_3C in Fe(C) capsules, fcc Co(C) in Co(C) capsules and bcc Fe–Co alloy in Fe–Co(C) capsules. This is supported by the XRD spectra of these capsules (figure 2). It is apparent that alloying Co into Fe can stabilize the bcc phase. The interface between the graphitic shell and the core is very sharp, showing that there is no intermediate phase. According to HRTEM observation, the bcc α-Fe(C) and orthorhombic Fe_3C in Fe(C) capsules are usually in different particles with small particle size. In some cases, they can coexist in one particle with a large particle size. It is clear that there is no particle with a shell of Fe_3C.

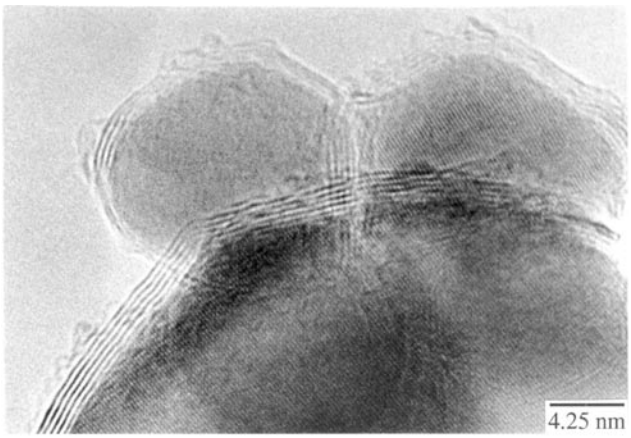

(a)

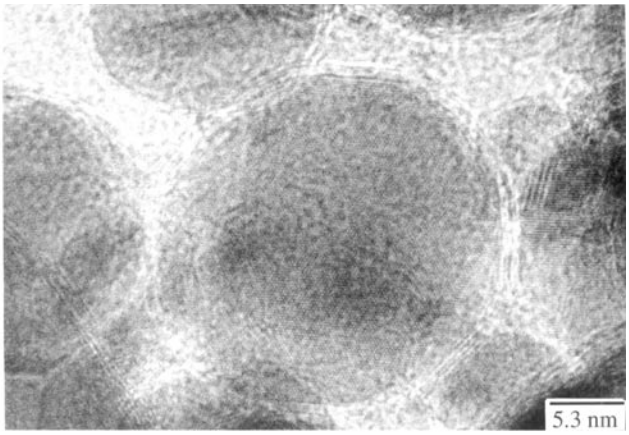

(b)

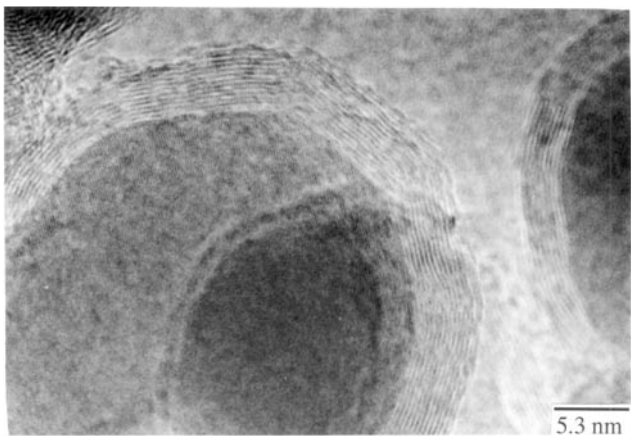

(c)

Figure 1. HRTEM images showing the shell–core structure of (a) Fe(C), (b) Co(C) and (c) Fe–Co(C) nanocapsules.

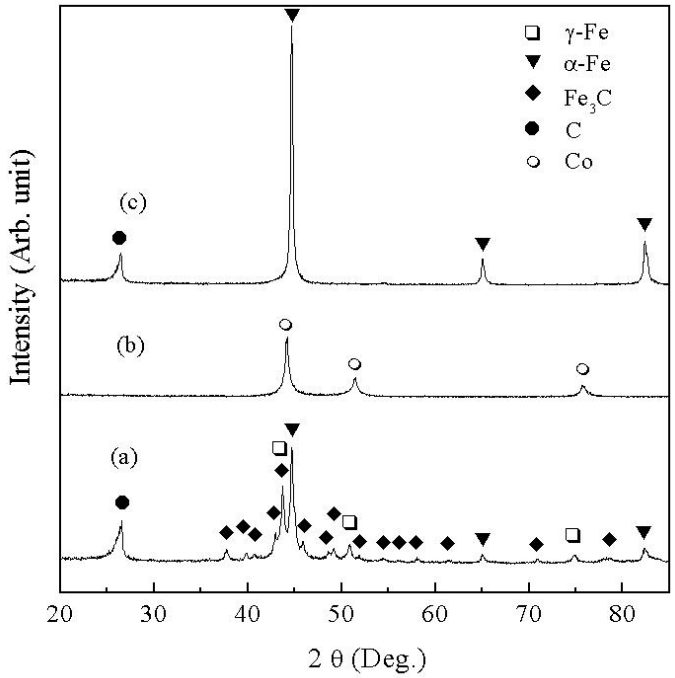

Figure 2. X-ray diffraction spectra of (a) Fe(C), (b) Co(C) and (c) Fe–Co(C) nanocapsules.

Particle sizes range from 10 nm to 100 nm, from 4 nm to 50 nm and from 10 nm to 170 nm as measured from HRTEM images of Fe(C), Co(C) and Fe–Co(C) capsules, respectively. It is obvious that the anode materials play an important role in the evaporation and condensation process and consequently also in determining the particle sizes.

The low-magnetic-field temperature-dependent magnetization has been measured in zero-field-cooled (ZFC) and field-cooled (FC) processes in order to obtain the energy barrier distribution (or size distribution) [11]. The procedure for the ZFC–FC magnetization measurement is as follows. The samples were first cooled in zero field to 5 K; then a magnetic field of 0.01 T or 0.1 T was applied to the samples. After that, the magnetization was measured in the warming process up to 350 K; thus the ZFC magnetization curve was obtained. The FC magnetization was measured while cooling the sample to 5 K with the same field. Figure 3 shows the ZFC–FC magnetization curves of Fe–Co(C) nanocapsules. The ZFC magnetization increases with temperature rapidly in two temperature ranges, from 5 to 75 K and from 300 to 350 K, but linearly between 75 and 300 K. Since the typical single-domain sizes of iron and cobalt for spherical shape are about 14 nm and 70 nm, respectively [9], and the upper limit of the particle sizes in our samples is about 170 nm, each temperature range may be associated with different mechanisms of magnetic alignment. Below 75 K, the relatively sharp increase of the ZFC magnetization may be due to some small particles with their blocking temperature falling in this temperature range. The blocking temperature T_B can be determined from $25k_BT_B = KV$, where KV is the anisotropy energy barrier; K and V are the effective anisotropy constant and the volume of particle, respectively [10–12]. The anisotropy at room temperature of pure cobalt (4.12×10^5 J m^{-3}) is almost one order larger than that of pure iron (4.81×10^4 J m^{-3}) and the large anisotropy of the former is attributed to its low-symmetry hexagonal structure. The Fe–Co(C) nanocapsules in the present work were

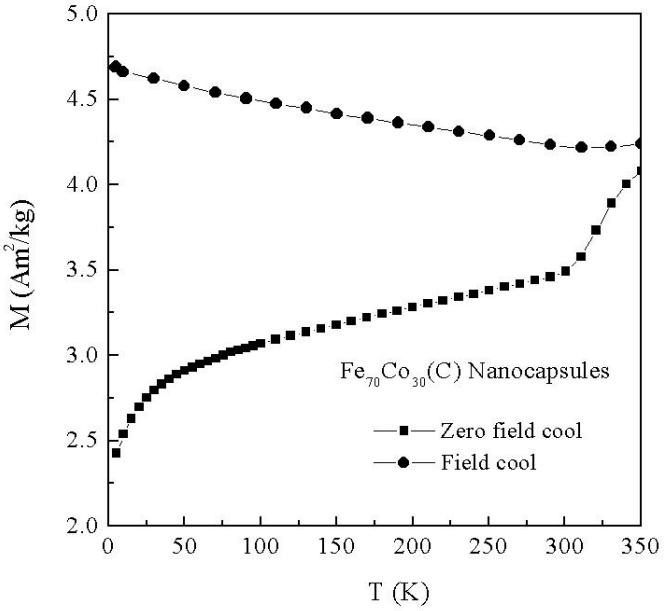

Figure 3. Zero-field-cooled (ZFC) and ($B = 0.01$ T) field-cooled (FC) magnetization curves of Fe–Co(C) nanocapsules.

prepared by evaporating $Fe_{70}Co_{30}$ alloy, which has the same cubic structure as the pure iron. The anisotropy of the $Fe_{70}Co_{30}$ alloy is close to that of the pure iron. Thus we can estimate the upper limit of the diameter of these small particles $D = 9$–11 nm by using $K = 5.4 \times 10^4$ J m^{-3} which is the anisotropy constant around liquid-He temperature for pure Fe. As shown above, the particle size ranges from 10 nm to 170 nm, measured from HRTEM images of Fe–Co(C) nanocapsules. The average shell thickness of Fe–Co(C) capsules is 3.4 nm. Therefore, the lowest value for the size of the magnetic cores in the Fe–Co(C) capsules should be about 3 nm. From the magnetic behaviours at low temperatures, we estimate the upper limit of the diameter of the small particles to be $D = 9$–11 nm. The upper limit of 'small particles' estimated from the magnetization is higher than the lower limit of the size of the magnetic cores observed by TEM. Thus, it can be concluded that the small particles which are responsible for the relatively sharp increase of the ZFC magnetization have been observed. However, it is difficult for us to reach a conclusion as to how many would be needed to account for the effect observed. We estimate that at least a 10% volume fraction is necessary for showing the unusual phenomena observed.

In the temperature range from 75 K to 300 K, there may still be a contribution of single-domain particles with a blocking temperature, but the linear increase of the magnetization with temperature can be mainly ascribed to the depinning of domain walls in multidomain particles [10–12]. When a small field is applied to multidomain particles at a low temperature, the domain structure changes immediately to a critical state, which is determined by the pinning barrier to the domain walls. Then the magnetization increases slowly, i.e. by a long-time relaxation process. The relaxation process is due to the depinning of domain walls caused by the thermal agitation. The barriers can be due to the structural imperfections in the particles. The sharp increase at 300 K can be considered as due to the particles with blocking temperature higher than 300 K. Similarly, the lower limit of the size for this group of particles can be

estimated: $D = 17$ nm, which is in agreement with HRTEM analysis. Measurements in the temperature range above 350 K are necessary for obtaining the distribution of the size or the energy barrier of the particles.

Although there are effects from the surface layers and from defects inside the particles, to simplify consideration one could neglect these effects and treat the contribution to the measured total magnetization by a particle as approximately proportional to the volume of its magnetic core, e.g. $M \propto D^3$. On this basis, the magnetization for 100 particles each with a 5 nm core diameter is approximately the same as that for a large particle with a 20 nm core diameter. Consequently, the overall behaviour of the magnetization for our samples will be dominated by the very large, multidomain particles—for example, the $M(T)$ data in the temperature range 75 K to 300 K. Only when rotating the magnetic moment coherently for the small particles is the behaviour of $M(T)$ dominated by the small particles—e.g. $M(T)$ at 300 K to 350 K.

Figure 4 shows zero-field-cooled (ZFC) and field-cooled (FC) magnetization curves of Fe(C) nanocapsules between 5 and 250 K. The ZFC magnetization increases with temperature rapidly from 5 to 30 K and smoothly from 50 to 250 K. There is a peak around 30 K. This peak can be ascribed to a group of Fe particles with a volume distribution whose blocking temperatures are around 30 K. It is evident that the number of particles whose blocking temperatures are about 30 K is much larger than that for Fe–Co samples. Actually the ZFC curve can be considered as the sum of a typical ZFC curve with a blocking temperature of about 30 K and the ZFC curve originating from the magnetic domain wall depinning in multidomain particles. Since the contribution to the total magnetization changes from the small single-domain particles is larger than that from domain wall depinning in multidomain particles in the temperature range from 5 K to 50 K, the peak at 30 K is quite prominent, which is similar to the case for the peak at (or above) 350 K in Fe–Co systems (figure 3). Similarly to the case for the Fe–Co(C) nanocapsules, the small particles have been observed by means of HRTEM for the Fe(C) nanocapsules.

One may note that the linear parts of $M(T)$ for the Fe–Co (figure 3) system and the Fe system (figure 4) are quite similar, but with different slope. The slope of the linear part of the $M(T)$ curve in figure 3 is larger than that of figure 4. This can be explained as due to

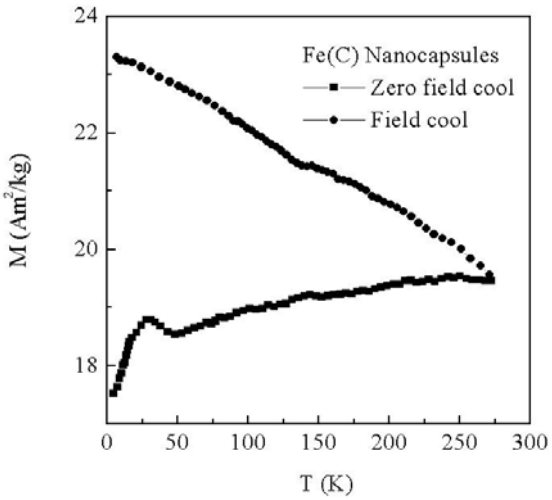

Figure 4. Zero-field-cooled (ZFC) and ($B = 0.1$ T) field-cooled (FC) magnetization curves for Fe(C) nanocapsules.

the different applied magnetic fields. In Fe–Co systems the applied field is 0.01 T, which is ten times less than the 0.1 T applied to the Fe system. Since the field of 0.1 T applied to the Fe system is quite large, it can overcome most small pinning barriers, and set the domain configuration much nearer the saturation configuration. Therefore, the relative increase in magnetization caused by domain wall depinning due to the thermal agitation with increasing temperature (ZFC) is smaller than that in the situation where the increase in magnetization with increasing temperature is due to the domain wall depinning through the small barriers.

Figure 5 shows the hysteresis loop of Fe–Co(C) nanocapsules at 350 K. The shapes of the hysteresis loops at lower temperatures are similar, except for the larger saturation magnetization and coercivity that increase with decrease of the measuring temperature. It is noted that the saturation magnetization is 98.6 A m^2 kg^{-1}, which is less than half of that for the pure bulk Fe. This is due to a large amount of carbon in the nanocapsules.

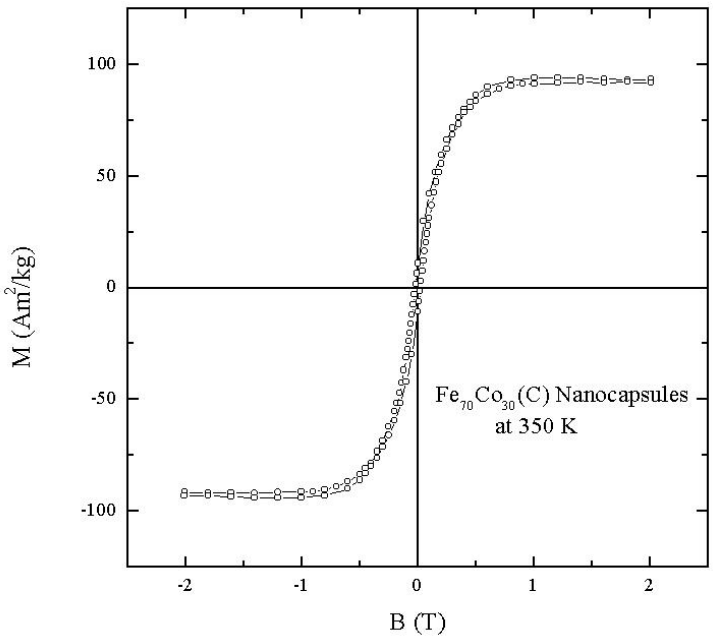

Figure 5. The hysteresis loop at 350 K of Fe–Co(C) nanocapsules.

Temperature dependencies of the magnetizations of Fe(C) and Fe–Co(C) nanocapsules are shown in figures 6(a) and 6(b). The magnetization, for both kinds of nanocapsule, decreases monotonically with increasing temperature. This behaviour is similar to that of the bulk materials. No spin-reorientation transition is found in these magnetization curves. The higher magnetization of the Fe–Co(C) nanocapsules, compared to that of the Fe(C) nanocapsules, is ascribed to the effect of alloying with cobalt, increasing the magnetization of the Fe–Co(C) nanocapsules, and also to the existence of the FeC_3 phase reducing the magnetization of Fe(C) nanocapsules. Figures 7(a) and 7(b) give the temperature dependences of the of Fe(C) and Fe–Co(C) nanocapsules; these coercivities drop significantly with increasing temperature. The coercivity of Fe(C) at 5 K is higher than that of Fe–Co(C) nanocapsules. But the coercivities of the two samples are very close at room temperature. The coercivity of the nanocapsules is about 0.02 T at 350 K and is almost two orders of magnitude higher than that of the corresponding bulk material.

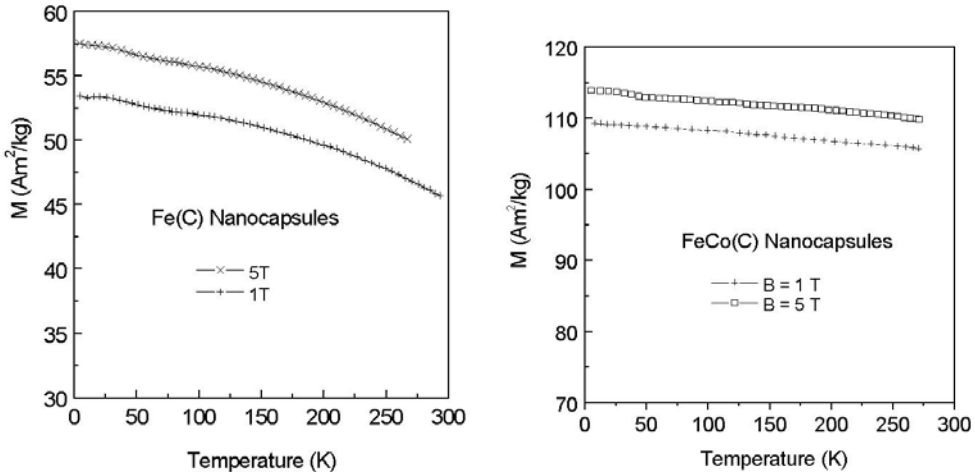

Figure 6. The temperature dependence of the magnetization of (a) Fe(C) and (b) Fe–Co(C) nanocapsules.

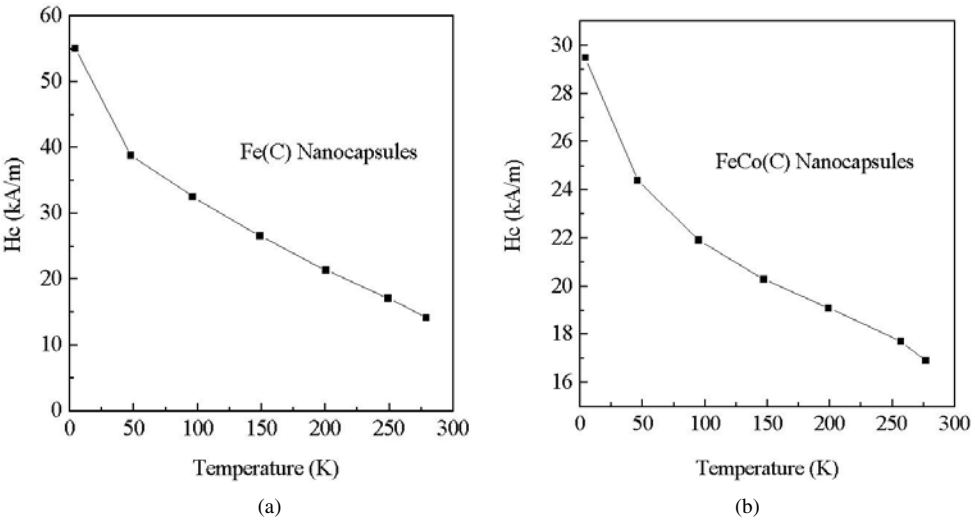

Figure 7. The temperature dependence of the coercivity of (a) Fe(C) and (b) Fe–Co(C) nanocapsules.

4. Summary

In summary, we have demonstrated in detail shell–core structures of the Fe(C), Co(C) and Fe–Co(C) nanocapsules prepared by arc discharge in a mixture of methane and helium. Three types of temperature dependence of the magnetization have been found in the ZFC M–T curve for the Fe–Co(C) nanocapsules. All of these magnetization behaviours can be interpreted in terms of the unblocking of the magnetization of the small single-domain particles and the depinning of the large multidomain particles. The saturation magnetization of these nanocapsules decreases monotonically, while the coercivity decreases significantly with increasing temperature.

Acknowledgments

This work was supported by the National Natural Science Foundation of China under grant No 59725103, and the Sciences and Technology Commission of Shenyang and Liaoning. It was also supported by Hong Kong RGC No HKUST6111/98P, by the NW STEM HB601 and JEM-2000EX at the University of Liverpool, and by VEGA under project 2/5141.

References

[1] Kroto H W, Heath J R, O'Brien S C, Curl R F and Smalley R E 1985 *Nature* **318** 162
[2] Krätschmer W, Lamb L D, Fostiropoulos K and Huffman D R 1990 *Nature* **347** 354
[3] Iijima S 1991 *Nature* **354** 56
[4] Iijima S and Ichihashi T 1993 *Nature* **363** 603
[5] Bethune D S, Kiang C H, de Vries M S, Gorman G, Savoy R, Vazquez J and Beyers R 1993 *Nature* **363** 605
[6] Ruoff R S, Lorents D C, Chan B, Malhotra R and Subramoney S 1993 *Science* **259** 346
[7] Dong X L, Zhang Z D, Chuang Y C and Jin S R 1999 *Phys. Rev.* B **60** 3017
[8] Dong X L, Zhang Z D, Jin S R and Kim B K 1999 *J. Appl. Phys.* **86** 6701
[9] Leslie-Pelecky D L and Rieke R D 1996 *Chem. Mater.* **8** 1770
[10] Zhang X X, Hernandez J M, Tejada J, Sole R and Ruiz X 1996 *Phys. Rev.* B **53** 3336
[11] Zhang X X, Tejada J, Hernandez J M and Ziolo R F 1997 *Nanostruct. Mater.* **9** 301
[12] Tejada J, Ziolo R F and Zhang X X 1996 *Chem. Mater.* **8** 1784